Effect of Volcano-like Textured Coated Tools on Machining of Ti6Al4V: An Experimental and Simulative Investigation

Yun Zhou
Jiangsu University
Yonghong Fu (fyh_ujs@163.com)
Jiangsu University
Jie Yang
Jiangsu University

Research Article

Keywords: FEM modeling , Ti6Al4V , volcano-like texture , chip morphology , tool wear

Posted Date: July 28th, 2021

DOI: https://doi.org/10.21203/rs.3.rs-747023/v1

Effect of volcano-like textured coated tools on machining of Ti6Al4V: an experimental and simulative investigation

Yun Zhou, Yonghong Fu, Jie Yang

School of Mechanical Engineering, Jiangsu University, Zhenjiang, Jiangsu, China, 212013

Corresponding Author/Email:fyh@ujs.edu.cn/TEL: +86-135-0528-2285/FAX:0511-88780056

Abstract: In this work, the main aim is to reduce the adhesion and wear that happened during machining of the Ti6Al4V alloy by employing volcano-like texture on the rake face of coated tool. A combination of experimental and simulative investigation was adopted. DEFORM-3D software with updated Lagrangian formulation was used for numerical simulation, and the thermo-mechanical analysis was performed using Johnson-Cook material model to predict the cutting temperature, cutting forces, chip morphology and tool wear. In cutting experiments, volcano-like textures with different area densities (10%, 20%, 30%) were fabricated by fiber laser on the rake face of cemented carbide tools close to the main cutting edge. Then, these textured tools were deposited with CrAlN coating through cathodic vacuum arc ion plating technique. Experiments in cutting Ti6Al4V alloy were carried out with the textured coated tools and non-textured coated tool under dry and wet cutting conditions. Then, the chip morphology, chip size and tool wear were investigated. The results showed that textured coated tools were superior to conventional tool. Especially in wet cutting, compared with those of non-textured coated tool, the adhesion area and the chip curling radius of the coated tool with texture area density of 20% (VCT2) were reduced by 31.2% and 49.7%, respectively. Therefore, VCT2 tool showed a better cutting performance. Finally, the mechanisms of textured coated tools under dry and wet cutting conditions were proposed.

Keywords FEM modeling · Ti6Al4V · volcano-like texture · chip morphology · tool wear

1 Introduction

With the characteristics of low density, high strength and corrosion resistance, Ti6Al4V alloy are an important material in aerospace, shipbuilding and chemical industries. Nevertheless, these factors lead to poor machinability of Ti6Al4V alloy due to its small elastic modulus, high chemical reaction activity and low thermal conductivity[1]. A lot of heat generated is confined over the tool-chip interface during the machining process[2]. This results in high cutting temperature that in turn facilitates the chip adhesion on the rake face of the tool. In addition, high contact stress in cutting Ti6Al4V alloy makes adhesive wear more likely to occur, which will shorten the service

life of the tool. Therefore, it is necessary to reduce the heat generated and friction at the interface in favor of the reduction of adhesion and wear on the rake face of the tool.

Laser surface texturing (LST) can improve tribological properties between contact surfaces, and has been successfully used in engineering fields such as bearings[3], mechanical seals[4], cylinder liner[5], etc. Attempts at extending this concept to cutting tool may be also a promising method to enhance the cutting performance. This enhancement is attributed to several mechanisms such as the reduction in the contact length/area between the two surfaces[6,7], wear debris entrapment[8] and the formation of micro-pool reservoir[9]. These mechanisms related with textured tool assist in lowering adhesion, wear and ploughing over the tool surface. Machado et al.[10] reviewed the research progress of textured tools from 2016 to date and related preparation technologies. The summary of previous works showed that the concave textures (mainly including pits and linear grooves) played a significant role in improving the cutting force, cutting temperature, tool life and cutting quality of workpiece. The properties of micro-textured tools predominantly depend on its topography on the surface. Therefore, many scholars attempted at designing and fabricating various functional microstructures on the tool surface. Darshan et al.[11] fabricated pitted textures on the surface of a cemented carbide (WC/Co) tool using a diode-pumped fiber. The textured tool reduced the contact area during the cutting process and enhanced the effectiveness of heat transfer compared with that of the non-textured tool, which significantly restrained the cutting force, cutting temperature and tool surface wear. Mishra et al.[12] studied the effect of varied shapes and area densities of chevron texture on tool performance of cutting titanium alloy. A combination of three-dimensional simulation and cutting experiments was performed, and it suggested that the volcano-like texture shapes had little effect on the cutting force, which, however, was sensitive to the texture area density. Further, the authors established the linear regression model for tool-chip contact length and found the reduction of tool-chip contact length was an important mechanism for better effectiveness of textured tools.

However, studies have shown that convex textures exhibit a better anti-adhesion effect by comparing with the concave textures[13]. Convex textures mainly incorporate the volcano-like, spherical crown convex and W-shaped textures, which are composite textures with concave and convex morphology. Kang et al. [14]imitated the surface morphology of animal skin and prepared volcano-like texture and groove on the rake face of cemented carbide tool. The cutting force, cutting stability, chip morphology, adhesion and wear of the tool were analyzed. It was concluded that lower cutting force and less adhesion can be observed by the volcano-like textured tool. To further understand the mechanisms of convex texture. Ma et al.[15] combined simulation and experiment to investigate the effects of different texture parameters (width, depth and the distance between the textures and edge) on the machining performance of the tool.

Results proved that the micro-bump textured tools can decrease the contact length between the tool and the chip, thereby reducing the cutting force as well as the energy consumption required for machining. Yu et al.[16] conducted a two-dimensional simulation of the cutting process of volcano-like textured tool under the condition of cutting fluid lubrication. This work revealed the cutting mechanism of textured tools under the conditions of cutting fluid lubrication and solved the problem of tool weakness. Through the analyses of the above literatures, the introduction of convex texture reduced the adhesion and wear, which greatly extended the service life of the tool. However, defects also are existed on the textured tool. Once the textures are filled or destroyed, the anti-adhesion effect of the textured tool will be invalid, so other methods are needed to be introduced. Commonly known protective coating is an indispensable component of high-performance cutting tools[17]. Hard coating, such as CrAlN, TiAlN, etc., is deposited on the surface of the tool to ensure the wear resistance and high temperature resistance, which has been highly recognized in the industries[18]. Thus, hard coating can also be used to protect the textured surface of the tool. Zhang et al.[19-21] have been committed to investigating the combination of texture technology and coating technology for many years, they comprehensively evaluated the cutting performance of the textured coated tools and found that textures lead to a significant enhancement in the cutting performance of coated tools, showing the reductions in cutting forces, cutting temperatures, friction coefficient and tool wear compared with that of the conventional coated tool. Further, the synergistic effects of textured coated tools were proposed by the machining processes and scratch experiments. Textures improved the adhesion strength between the coatings and the substrate, meanwhile, hard coating also protected the surface morphology of the textures, which reduced tool wear and extended the service life.

Thus, we intended to explore the effect of the combination of volcano-like texture and hard coating on the cutting performance of the tool in this work. Experimental and simulative investigation was carried out. Firstly, a volcano-like texture was designed on the rake face of cemented carbide tool. The cutting simulation software DEFORM-3D was used to investigate the tool performance in cutting force, cutting temperature, chip morphology, tool adhesion and wear. Then experiments of machining Ti6Al4V were conducted to compare the FEM model under different texture densities, cutting speeds and cooling conditions. Finally, the mechanisms of the cutting performance of textured coated tools were to be discussed, which will contribute to the design and manufacturing methods of textures on the tool surface.

2. Simulation of the machining process

2.1 Finite element mode for machining

In this study, DEFORM-3D was selected to simulate the machining process based

on updated Lagrangian formulation with cemented carbide cutting tool. The cutting performance of four kinds of tools was explored at different cutting speeds. The 3D FEM cutting model of tool and workpiece for simulation is exhibited in Fig. 1. As Fig. 1 described, it can be clearly seen that the tool moved around the fixed workpiece.

The non-textured tool and volcano-like textured tools were designed with SolidWorks according to the real shape and size of cutting tool and then imported into DEFORM-3D. After that, all cutting tools were endowed CrAlN hard coating established. The cutting tools and workpiece were meshed and ranged from 183516~202000 and 41515 elements by adaptive meshing technique that ensured the accuracy of simulation model and the reduction of calculation. To simplify nomenclature, the designed tool which was coated CrAlN without textures was named NCT. The designed tool which was coated CrAlN with volcano-like texture (convex texture) was denoted as VCT and different densities (10%, 20%, 30%) were named as VCT1, VCT2 and VCT3, respectively. The three-dimensional shape and related parameters of the four tools are shown in Fig. 2 and Table1, respectively.

2.2 J-C model for workpiece material

Ti6Al4V alloy was selected as the workpiece material. For getting finer mesh density, workpiece was represented as a curved model with a radius of 60mm and curvature angle of 20° with fixed bottom constraints in all directions. There are a variety of constitutive equations describing material properties in DEFORM-3D, such as Johnson-Cook constitutive model, Zerilli-Armstrong constitutive model, Bodner-Partom constitutive model, etc. Johnson-Cook constitutive model can better reflect the strain hardening, strengthening and thermal softening effects of the workpiece material, which is more in consistent with the actual cutting process. Empirical formula of the model can be written as:

$$\bar{\sigma} = [A + B(\bar{\varepsilon})^n]\left[1 + Cln\left(\frac{\dot{\bar{\varepsilon}}}{\dot{\bar{\varepsilon}}_0}\right)\right][1 - (\frac{T-T_r}{T_m-T_r})^m] \quad (1)$$

where $\bar{\sigma}$ is the equivalent stress, A, B, and C are material yield stress, hardening modulus and strain rate dependency coefficient, respectively; n is strain hardening index and m is temperature strain sensitivity coefficient; T_r, T_m and T represent the room temperature, the melting temperature and the operating temperature, respectively. $\dot{\bar{\varepsilon}}$ is the effective plastic strain rate and $\dot{\bar{\varepsilon}}_0$ is the reference strain rate. The values of mechanical properties and constitutive model parameters for Ti6Al4V are listed in Table 2[22,23].

3. Experimental details

The cutting experiments were carried out with Ti6Al4V alloy in the form of a

round bar with a radius of 30mm and length of 100mm selecting cemented carbide (YG3). The volcano-like texture was fabricated on the tool rake face by Raycus RFL C500 fiber laser (1080nm wavelength, 500W) with the processing parameters as described in Table 3. Under the conditions of a laser re-melting process, a laser with high energy and long pulse width was injected into the local zone of the tool. Driven by the gradient surface tension and the flow of local molten pool generated by laser radiation, a volcano-like texture with a composite morphology with a certain height of raised edge bulge and central depression was obtained[24,25]. Then a layer of 2μm CrAlN hard coating was deposited on the surface of textured tool using the cathodic vacuum arc ion plating technique. Fig. 3 shows four types of cutting tools and morphology of volcano-like texture. The surfaces of the textured tools were measured using an upright optical microscope (Leica DM750) and an ultra-depth-of-field electron microscope (VHX-2000C).

Machining experiments were conducted on an engine lathe (CS6140), using the tool holder with the following parameters: rake angle γ_o = 6°, clearance angle α_o = 6°, inclination angle λ_s = -7.2°. Machining conditions are shown in Table 4. The worn surfaces of the tool and chip morphology were observed by scanning electron microscope (SEM).

4. Results and discussion

4.1 Cutting temperature

High cutting temperature is one of the main reasons for tool wear that directly affects cutting quality and the tool life. The elastoplastic deformation of the primary and secondary deformation zones and the friction on the tool-chip/workpiece interface are the main sources of cutting heat, which is predominately dissipated by the chip[26]. In the present study, the cutting temperature on the chip was investigated.

Fig. 4 shows the temperature distribution on the chip produced by four types of cutting tools at 120m/min. The initial temperature of the operation environment was set as 25℃. When the cutting process reached to a steady state, NCT tool had the highest cutting temperature (1030°C) that was mainly distributed in the contact part with the rake face of the tool compared with that of VCT tools. For VCT1, VCT2 tools, the highest cutting temperatures were 985°C, 924°C, respectively, which were lower than that of NCT tool at the same cutting speed. This can be explained as the volcano-like texture promoted the bending of the chip and reduced the contact area between the tool and the chip. Furthermore, the textured tool created a vacuum in the area where the chip was in close contact with the tool surface, which decreased the heat concentration on the tool surface. The volcano-like texture outside the tool-chip contact area increased the convective heat transfer area between the tool surface and the air, so that the heat can speed up the heat transfer. When the texture occupancy rate reached to 30%, the

cutting temperature was reduced by 6.0% compared with that of NCT tool, However, the cutting temperature was increased by 4.8% compared with VCT2 tool. It was possible that high texture area density may weaken the strength of the tool, thereby increasing the wear on the tool surface, which in turn increased the generation of cutting heat.

In general, it can be seen that the volcano-like texture could improve the tribological state at the tool-chip interface and reduce the generation of cutting heat, but the texture area density needs to be controlled within a certain range.

4.2 Cutting forces

The main cutting forces of NCT and VCT tools observed during machining simulation of Ti6Al4V for different cutting speeds are shown in Fig. 5(a). In general, compared with that of NCT tool, VCT tools could reduce the main cutting force for any given cutting speeds. From Fig. 5(a), a maximum main cutting force of 190.41N was observed for the NCT tool at the cutting speed of 60 m/min. Compared with that of NCT tool under the same cutting conditions, the main cutting forces of VCT1, VCT2 and VCT3 tools were reduced by 7.6%, 9.1% and 4.4%, respectively, indicating that the introduction of volcano-like texture lowered the main cutting force. Among all cutting tools, it was observed that the main cutting force of VCT2 tool was the minimum(173N), which illustrated that the texture area density had optimal value in the simulation results. When the cutting speed increased from 60 to 120 m/min, a main cutting force of 169.35 N was observed with NCT tool and 150 N for VCT2 tool under the simulative conditions. The reduction in the main cutting force as the increasing speed is due to greater chip plastic deformation and reduced friction on the tool-chip/workpiece contact interface, and the chip is softened by the continuous cutting heat generated [27].

The radial forces of NCT and VCT tools observed during machining simulation of Ti6Al4V for different cutting speeds are shown in Fig. 5(b). The maximum radial force of 87.1N was noticed with NCT tool at the cutting speed of 60m/min. Under the same machining conditions, the minimum radial force of 73.2N was found with VCT2 tool, which was 16.0 % lower than that of NCT tool. The reduction in radial force can be attributed to shorter tool-chip contact length/area and better heat dissipation area for textured coated tool. With the cutting speed increasing from 60 to 120 m/min, the radial force of VCT2 was reduced by 16.3% compared to NCT tool.

From the simulation results, it can be seen that as texture area density on the rake face increased, the radial forces for VCT tools decreased initially, and then increased. This was similar to the conclusion obtained from the spherical texture mentioned in literature [28]. Therefore, it is believed that the density of the volcano-like texture has a great influence on the performance of the tool, which will be further analyzed in the

following sections.

4.3 Chip morphology

Fig. 6 depicts the chip generated by the four cutting tools under the simulative conditions at 120m/min. It can be clearly seen from Fig. 6 that at step 1290, the chip back of the NCT tool was smoother than that of VCT tools. Regular micro-grooves pointed by the green arrow were found on the chip back of the VCT tools, which were a print effect of the convex part of the volcano-like texture. The above phenomena illustrated that in the tool-chip contact process, the volcano-like texture generated an inward torque to the chip and promoted chip bending. Therefore, the spiral chip with smaller radius was obtained.

Fig. 7 shows the chip of four kinds of tools when the cutting speed is 120m/min under the dry and wet cutting conditions. Friction between the tool-chip contact interface is an important factor affecting the chip formation, such as size, surface topography. Less friction at the contact zone facilitates the smaller radius curled chip[11] . From Fig. 7, the curled radius of the chip produced by the NCT tool was the largest in dry cutting, which was difficult to break and thus increased the frequency of chip entanglement with the workpiece or the tool. Compared with that of VCT tools, NCT tool had the largest tool-chip contact length/area, resulting in more friction. Under wet cutting conditions, VCT tools obtained the chips with a smaller radius compared with that of NCT tool, which indicated that a lubricant film was formed between the rake face of the cutting tool and the chip. As a result, the lubricant film helped in the reduction of the friction and shear force between the two contact surfaces, promoting the bending of the chips and the chip-breaking efficiency. From Fig. 4, it can be found that the convex morphology of the volcano-like texture was relatively mild. Hence the texture may play a role in holding up the chips when the chips slid across the tool rake surface, reducing the tool-chip contact length/area.

Fig. 8-11 show the SEM images of the chip free surface when the cutting speed is 120m/min. R means the curl radius of the chip measured with imagej software and shown in Table 5. It was observed that under dry cutting conditions, the chip with continuous straight shape and the maximum radius produced by NCT tool was observed. After adding cutting fluid, the chip generated was spiral crimp. Compared with that of NCT tool, the chip-curl radius produced by VCT1, VCT2 and VCT3 tools was reduced by 36.4%,49.7% and 25.6, respectively. Among all the tools, VCT2 tool produced the smallest chip radius under the two cutting conditions, which illustrated that the introduction of the volcano-like texture and the changes of the cutting environment had a great effect on a contact state between the tool and the chip.

In general, serrated chips were shaped at the primary and secondary surfaces in both wet and dry conditions in the process of machining Ti6Al4V due to unstable plastic

deformation with adiabatic shear. In the high-magnification images, it was found that chip free surface had a lamellar structure. The micro-defects on the workpiece material played a very important role in the formation of the lamellar structure. Due to the instability of the thermo-plastic flow micro-defects could appear in the shear surface, resulting in layer by layer slipping [29]. As the Fig. 8-11 described, the smoother free surface and less lamellar structures of NCT tool were observed compared with that of VCT tools. More friction was produced on the tool-chip interface and then caused high temperature, inhibiting the generation of lamellar structures of the NCT tool. In addition, the segmental chip space formed by VCT tools under wet cutting environment (considering the chip bending radius) was larger than that of dry cutting at the same speed and namely, the smaller segmentation frequency of chips[30]. With the increasing texture area density, this phenomenon became obvious. Therefore, compared with that of NCT tool, VCT tools had a smaller chip segmentation frequency. Since chip segmental frequency was associated with chip stability, VCT tools reduced vibrating in the tool system. In addition, the cutting fluid can help in alleviating the contact state on the too-chip interface, resulting in the more stable cutting process.

Fig. 12 shows the SEM images of the chip back surface of NCT and VCT2 tools at 120m/min. From the high magnification of Fig. 12, it can be found that the back surface of the NCT tool was relatively smooth, while there were uniform arc-shaped grooves on that of the chip generated by VCT2 tool. These traces indicated that the convex texture can support the chip, which promoted the chip curling and the material removal, resulting in additional deformation in the primary and secondary shear zones. These phenomena were consistent with the chip simulation results in Fig. 6.

4.4 Surface wear

Fig. 13 shows the wear depth of the rake face of the four types of cutting tools under the simulative conditions at 120m/min. Tool wear was concentrated at the rake face extending to the periphery in a gradient, and the area with highest wear degree was near the cutting edge. It was found that the wear tracks of VCT tools used in this study were similar with the NCT tool and the maximum wear depth was less than that of NCT tool. From Fig. 13 (b-d), the maximum wear of VCT1, VCT2, and VCT3 tools were 0.000421mm, 0.000413 mm, and 0.000430 mm, respectively. Therefore, the maximum wear of VCT2 tool was the smallest compared with that of NCT tool, which was reduced by 8.0%. In general, the introduction of texture reduced the surface wear of the tool under the simulative conditions, and VCT2 tool exhibited better wear resistance than other coated tools.

In order to further understand the wear mechanisms under simulative conditions, the worn surface of the tools after cutting experiment was studied. The large tool-chip contact length/area, high cutting temperature near the tool tip and lack of proper

lubrication will cause tool surface wear, which decreases the service life of the tool [31].

Fig. 14 shows the marks of adhesion area on the rake face of NCT and VCT tools. The adhesion area of NCT tool was obviously larger than that of VCT tool. According to Fig. 15, compared with that of the NCT tool, the tool-chip adhesion area of VCT1, VCT2 and VCT3 tools under dry cutting conditions were decreased by 8.6%, 17.4% and 9.7%, respectively. Therefore, it can be seen that VCT2 tool exhibited less surface adhesion and wear than other coated tools. When the cutting speed increased from 60 to 120m/min, adhesion area of the four types of cutting tools enlarged, with the area of NCT tool reaching to 81.8%. As the cutting temperature increased, more softened chips adhered on the surface of the tool. The cutting regions experienced a "formation–stacking–plucking" process. Due to this repetitive process, the workpiece material on the tool surface teared by the sliding chips, causing adhesion wear on the tool surface. In Fig. 16, the adhesion and wear of the rake face of the NCT tool was more obvious, while less wear on the surface of VCT2 tool was observed. This is because the existence of the volcano-like texture reduced the length of the tool-chip contact, and it can be seen that there was debris inside the concave part of the texture, which reduced the scratches on the tool surface.

Under wet cutting conditions, similar wear pattern appeared on the tool surface. At 60m/min, the adhesion area of the four types of cutting tools was reduced by 7.3%, 17.1%, 15.2%, and 7.7% compared with the dry cutting, respectively. The cutting fluid acted as not only a coolant but also a lubricant, which can help to carry away the debris formed in cutting process, alleviating the tribological state of the tool-chip contact surface and reducing the generation of cutting heat. In Fig. 17 (c, d), the volcano-like texture increased the air gap between the tool-chip interface, which can transmit the cutting fluid to the sticking and slip zones. Therefore, only a small amount of adhesion and wear on the tool surface was found.

4.5 Mechanisms for the effect of volcano-like texture coated tool

In this study, the cutting process of four textured coated tools was simulated by DEFORM-3D. The cutting surface temperature, cutting force, chip morphology and tool wear were predicted. The results illustrated that VCT tools had the potential to improve the cutting performance. Therefore, cutting experiments were carried out to further verify and explore the physical mechanisms of the textured coated tools in different cutting environments based on the simulation.

The friction between the tool rake face and the chip can be obtained by the following equation [32]:

$$F_f = A_r \tau_c \tag{2}$$

Where A_r is the actual tool-chip contact area, τ_c is the average shear strength at the tool–

chip interface.

The schematic diagram of the contact interface between the volcano-like textured coated tool and the non-textured coated tool with the chip is shown in Fig. 18. We found that the volcano-like texture is a composite morphology containing convex and concave regions. In dry and wet cutting, the contact area between the volcano-like texture and the chip is peak point contact, while the NCT tool is in a compact surface contact.Therefore, VCT tools are able to decrease the contact area A_r between the tool and the chip (Fig. 15) and improve the tribological performance of the tool-chip contact interface. As a result, the cutting temperature and cutting forces were reduced. Although the convex shape at the initial cutting process has a blocking effect on the chip , it can also support the chip and promote the curling of the chip. Experimental results have proved that the latter plays a dominate role.In addition, the volcano-like texture increases the heat ardiating area and accelerates the heat convection with air or cutting fluid, reducing the adhesion and wear on the rake face[15]. The chip mophology obtained by simulation and experiment (section 4.3) was found that the convex morphology printed micro grooves on the chip back. This phenomenon shows that the volcano-like texture acts as micro tool and increases the cutting efficiency. Under wet cutting conditions, cutting fluid also plays an important role in cooling and lubricating. The volcao-like texture can efficiently promote cutting fluid to penetrate into the tool-chip intimate interface. The concave part of the volcano-like texture can act as a micro-pool for the cutting fluid and entrap the debris generated during the cutting process.Thus VCT tools can reduce the damage to the tool surface and extend the service life.

Although the volcano-like texture produced on the rake face of tool can enhance the performance of the tool, it was also noticed that when the texture ratio was 30%, the cutting temperature, cutting force and chip curling radius were increased compared with that of VCT2 tool, so it is not the higher the texture ratio, the better the tool performance. From the perspective of tool surface wear, when the texture area density reaches a certain degree, the strength of the tool will be declined.

5. Conclusions

In this study, in order to study the effect of different densities of volcano-like textures on the cutting performance of CrAlN coated tools, FEM cutting simulation was firstly performed in DEFORM-3D software to predict the changes of cutting temperature, cutting force, chip morphology and tool wear. Then the dry and wet cutting experiments were carried out based on the results of simulation. The main conclusions are obtained as follows:

1. The simulation results showed that compared with that of NCT tool, the cutting temperature of VCT1, VCT2 and VCT3 tools were reduced by 4.4%, 10.3%, 6.0%,

respectively. At 60m/min, the main cutting forces were reduced by 4.4%-9.1% for VCT tools, and the radial force were reduced by 5.6%-16.0% compared with that of NCT tool. In addition, the cutting forces received by VCT tools were decreased as the cutting speed increased.

2. In the dry and wet cutting experiments, the volcano-like texture was fabricated on the rake face and then deposited with CrAlN coating by fiber laser and the cathodic vacuum arc ion plating technique, respectively. The experiment results show that compared with that of NCT tool, the obtained VCT tools increase the chip curling and reduce tool surface wear, and demonstrate better anti-adhesion effect.

3. Through simulative and experimental investigation, it is shown that texture area density has a great influence on the tool surface properties. And VCT2 tool exhibits better cutting performance than that of other cutting tools.

4. The physical mechanisms responsible for the improvement of cutting performance and tool wear are found. The volcano-like texture can reduce the tool-chip contact length/area and support the chip by the convex part, which results in decreasing the interaction between the chip and rake face and bending the chip. In wet cutting, the texture can be helpful in carrying and entrapping the cutting fluid and debris, thus reducing the damage of tool surface.

Acknowledgments

This work was supported by a grant from National Natural Science Foundation of China (No. 52075225), Zhenjiang Science and Technology Innovation Foundation (No. ZD2020004)

Institutional Affiliations

All affiliations are listed on the title page of the manuscript.

Funding

All funding sources for this study are listed in the “Acknowledgments” section of the manuscript.

Conflicts / Competing Interests

We declare that we do not have any commercial or associative interest that represents a conflict of interest in connection with the work submitted.

Availability of data and material

The datasets used or analyzed during the current study are available from the corresponding author on reasonable request.

Code availability

Not applicable.

Authors' contributions

Conceptualization: Yun Zhou, Yonghong Fu; Methodology: Yonghong Fu; Formal analysis and investigation: Yun Zhou; Writing - original draft preparation: Yun Zhou; Writing - review and editing: Yonghong Fu, Jie Yang; Funding acquisition: Yonghong Fu; Resources: Yonghong Fu; Supervision: Yonghong Fu.

References

1. Byrne G, Dornfeld D, Denkena B (2003) Advancing cutting technology. CIRP Ann-Manuf Technol 52:483-507. https://doi.org/10.1016/S0007-8506(07)60200-5
2. Pramanik A (2013) Problems and solutions in machining of titanium alloys. Int J Adv Manuf Tech 70(5-8):919-928. https://doi.org/10.1007/s00170-013-5326-x
3. Marian VG, Gabriel D, Knoll G, Filippone S (2011) Theoretical and experimental analysis of a laser textured thrust bearing. Tribol Lett 44(3):335-343. https://doi.org/10.1007/s11249-011-9857-8
4. Wang T, Huang W, Liu X, Li Y, Wang Y (2014) Experimental study of two-phase mechanical face seals with laser surface texturing. Tribol Int 72:90-97. https://doi.org/10.1016/j.triboint.2013.12.009
5. Sabri L, El Mansori M (2009) Process variability in honing of cylinder liner with vitrified bonded diamond tools. Surf Coat Technol 204(6-7):1046-1050. https://doi.org/10.1016/j.surfcoat.2009.05.013
6. Sugihara T, Enomoto T (2013) Crater and flank wear resistance of cutting tools having micro textured surfaces. Precis Eng 37(4):888-896. https://doi.org/10.1016/j.precisioneng.2013.05.007
7. Jianxin D, Ze W, Yunsong L, Ting Q, Jie C (2012) Performance of carbide tools with textured rake-face filled with solid lubricants in dry cutting processes. Int J Refract Met Hard Mater 30(1):164-172. https://doi.org/10.1016/j.ijrmhm.2011.08.002
8. Sugihara T, Enomoto T (2017) Performance of cutting tools with dimple textured surfaces: A comparative study of different texture patterns. Precis Eng 49:52-60. https://doi.org/10.1016/j.precisioneng.2017.01.009
9. Zhang K, Deng J, Xing Y, Li S, Gao H (2015) Effect of microscale texture on cutting performance of wc/co-based tialn coated tools under different lubrication conditions. Appl Surf Sci 326:107-118. https://doi.org/10.1016/j.apsusc.2014.11.059
10. Machado AR, Da Silva LRR, De Souza FCR, Davis R, Pereira LC, Sales WF, De Rossi W, Ezugwu EO (2021) State of the art of tool texturing in machining. J Mater Process Technol 293. https://doi.org/10.1016/j.jmatprotec.2021.117096
11. Darshan C, Jain S, Dogra M, Gupta MK, Mia M (2019) Machinability improvement in inconel-718 by enhanced tribological and thermal environment using textured tool. Journal of Thermal Analysis and Calorimetry 138(1):273-285. https://doi.org/10.1007/s10973-019-08121-y
12. Mishra SK, Ghosh S, Aravindan S (2018) 3d finite element investigations on textured tools with different geometrical shapes for dry machining of titanium alloys. Int J Mech Sci 141:424-449. https://doi.org/10.1016/j.ijmecsci.2018.04.011
13. Kang Z, Fu Y, Chen Y, Ji J, Fu H, Wang S, Li R (2018) Experimental investigation of concave and convex micro-textures for improving anti-adhesion property of cutting tool in dry finish cutting. Int J Precis Eng Manuf-Green Technol 5(5):583-591. https://doi.org/10.1007/s40684-018-0060-3
14. Kang Z, Fu Y, Fu X, Jun M (2018) Performance of volcano-like laser textured cutting tools: An experimental and simulative investigation. Lubricants 6(4). https://doi.org/10.3390/lubricants6040098
15. Ma J, Duong NH, Lei S (2015) Numerical investigation of the performance of microbump textured cutting tool in dry machining of aisi 1045 steel. J Manuf Process 19:194-204. https://doi.org/10.1016/j.jmapro.2014.10.001
16. Yu Q, Zhang X, Miao X, Liu X, Zhang L (2020) Performances of concave and convex microtexture tools in turning of ti6al4v with lubrication. Int J Adv Manuf Tech 109(3-4):1071-1092.

https://doi.org/10.1007/s00170-020-05656-5
17. Sedlaček M, Podgornik B, Ramalho A, Česnik D (2017) Influence of geometry and the seq uence of surface texturing process on tribological properties. Tribol Int 115:268–273. https://doi.org/10.1016/j.triboint.2017.06.001
18. Jianxin D, Jianhua L, Jinlong Z, Wenlong S, Ming N (2008) Friction and wear behaviors of the pvd zrn coated carbide in sliding wear tests and in machining processes. Wear 264(3-4):298-307. https://doi.org/10.1016/j.wear.2007.03.014
19. Zhang K, Deng J, Ding Z, Guo X, Sun L (2017) Improving dry machining performance of tialn hard-coated tools through combined technology of femtosecond laser-textures and ws2 soft-coatings. J Manuf Process 30:492-501. https://doi.org/10.1016/j.jmapro.2017.10.018
20. Zhang K, Deng J, Guo X, Sun L, Lei S (2018) Study on the adhesion and tribological behavior of pvd tialn coatings with a multi-scale textured substrate surface. Int J Refract Met Hard Mater 72:292-305. https://doi.org/10.1016/j.ijrmhm.2018.01.003
21. Zhang K, Deng J, Sun J, Jiang C, Liu Y, Chen S (2015) Effect of micro/nano-scale textures on anti-adhesive wear properties of wc/co-based tialn coated tools in aisi 316 austenitic stainless steel cutting. Appl Surf Sci 355:602-614. https://doi.org/10.1016/j.apsusc.2015.07.132
22. Mishra SK, Ghosh S, Aravindan S (2019) Performance of laser processed carbide tools for machining of ti6al4v alloys: A combined study on experimental and finite element analysis. Precis Eng 56:370-385. https://doi.org/10.1016/j.precisioneng.2019.01.006
23. Özel T, Sima M, Srivastava AK, Kaftanoglu B (2010) Investigations on the effects of multi-layered coated inserts in machining ti–6al–4v alloy with experiments and finite element simulations. CIRP Annals 59(1):77-82. https://doi.org/10.1016/j.cirp.2010.03.055
24. Du D, He YF, Sui B, Xiong LJ, Zhang H (2005) Laser texturing of rollers by pulsed nd:Yag laser. J Mater Process Technol 161(3):456-461. https://doi.org/10.1016/j.jmatprotec.2004.07.083
25. Inogamov N, Zhakhovsky V, Khokhlov V, Petrov Y, Migdal K (2016) Solitary nanostructures produced by ultrashort laser pulse. Nanoscale Research Letters 11. https://doi.org/10.1186/s11671-016-1381-1
26. Wu Z, Bao H, Liu L, Xing Y, Huang P, Zhao G (2020) Numerical investigation of the performance of micro-textured cutting tools in cutting of ti-6al-4v alloys. Int J Adv Manuf Tech 108(1-2):463-474. https://doi.org/10.1007/s00170-020-05428-1
27. Arulkirubakaran D, Senthilkumar V, Dinesh S (2016) Effect of textures on machining of ti-6al-4v alloy for coated and uncoated tools: A numerical comparison. Int J Adv Manuf Tech 93(1-4):347-360. https://doi.org/10.1007/s00170-016-9381-y
28. Zhang Y, Wang X, Li H, Wang B (2015) Adhesive behavior of micro/nano-textured surfaces. Appl Surf Sci 329:174-183. https://doi.org/10.1016/j.apsusc.2014.12.040
29. Rao CM, Rao SS, Herbert MA (2019) An experimental and numerical approach to study the performance of modified perforated cutting tools on machining of ti–6al–4v alloy. Arabian Journal for Science and Engineering 45(2):1191-1206. https://doi.org/10.1007/s13369-019-04268-w
30. Yang Q, Wu Y, Liu D, Chen L, Lou D, Zhai Z, Liu Z (2016) Characteristics of serrated chip formation in high-speed machining of metallic materials. Int J Adv Manuf Tech 86(5-8):1201-1206. https://doi.org/10.1007/s00170-015-8265-x
31. Sugihara T, Enomoto T (2012) Improving anti-adhesion in aluminum alloy cutting by micro stripe texture. Precis Eng 36(2):229-237. https://doi.org/10.1016/j.precisioneng.2011.10.002
32. Chen R (1985) Principle of metal cutting. China Machine Press, Beijing.

Figures

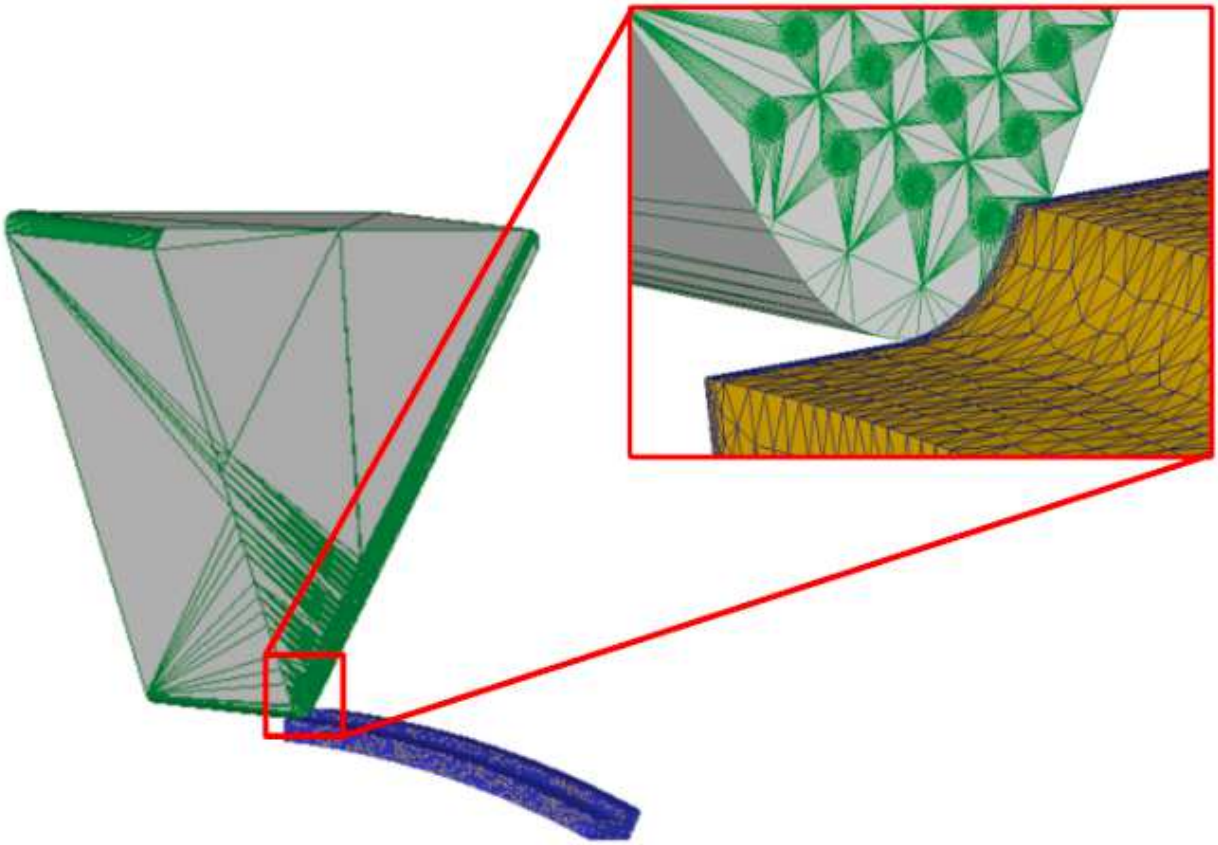

Figure 1

The finite-element modeling of cutting tool and workpiece

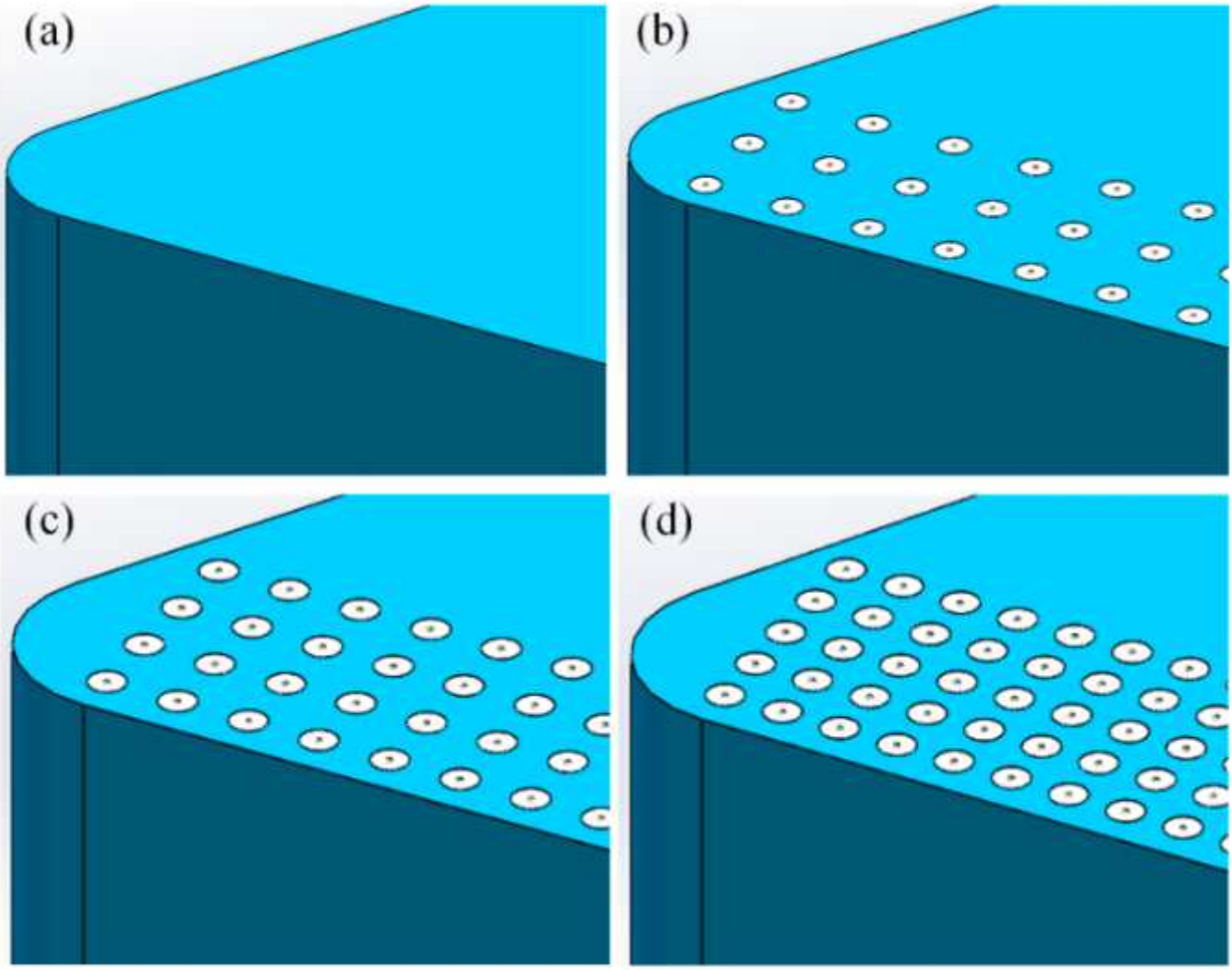

Figure 2

Three-dimensional model of NCT and VCT tools

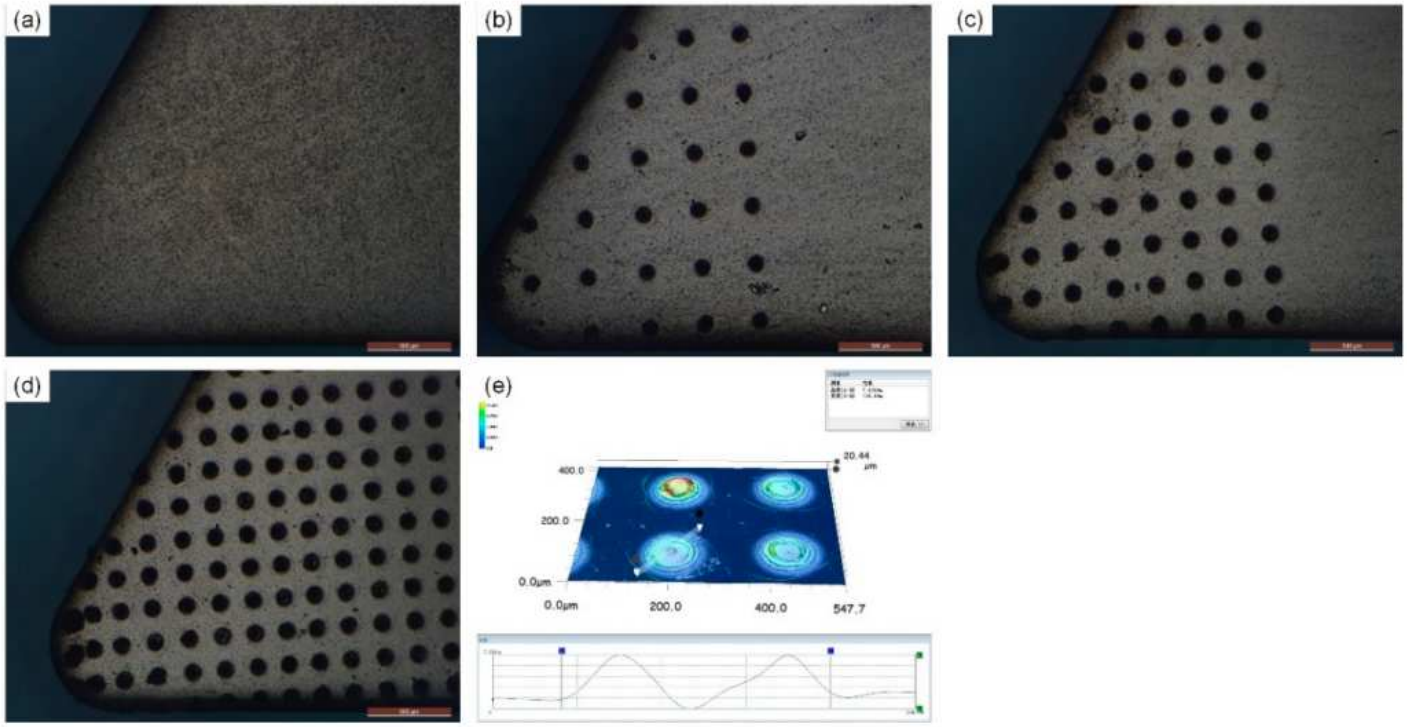

Figure 3

Four types of cutting tools (a-d) and morphology of volcano-like texture (e)

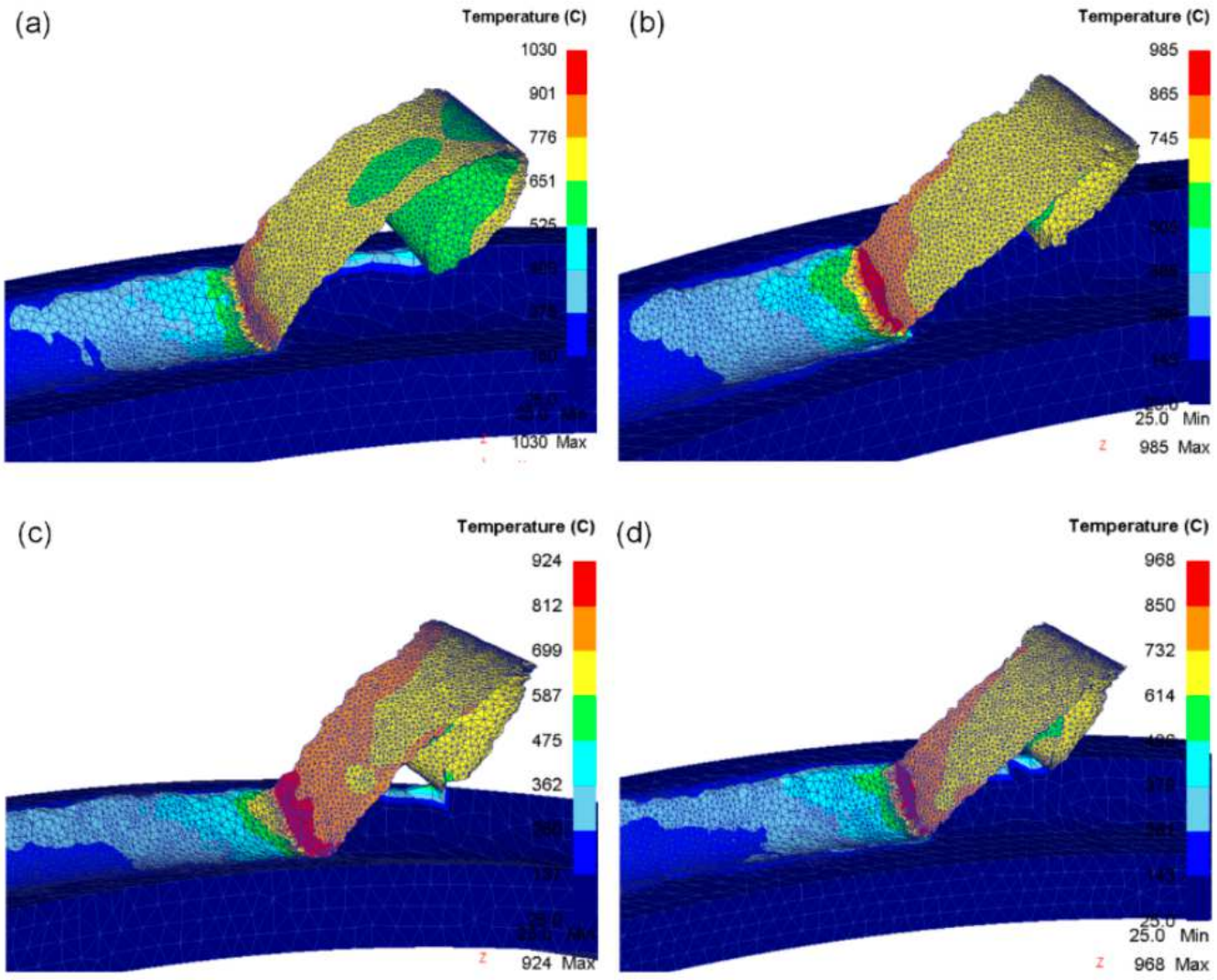

Figure 4

Temperature distribution on the chip produced by the NCT and VCT tools under simulative conditions

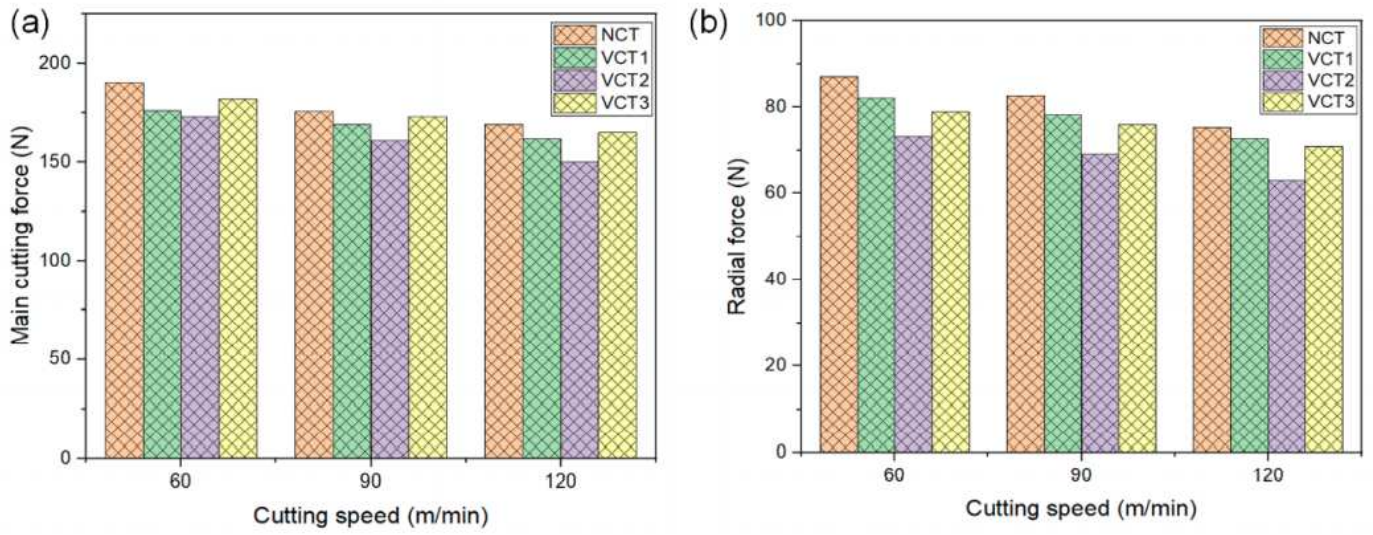

Figure 5

Main cutting force (a) and radial force (b) of four types of cutting tools in different speeds under simulative conditions

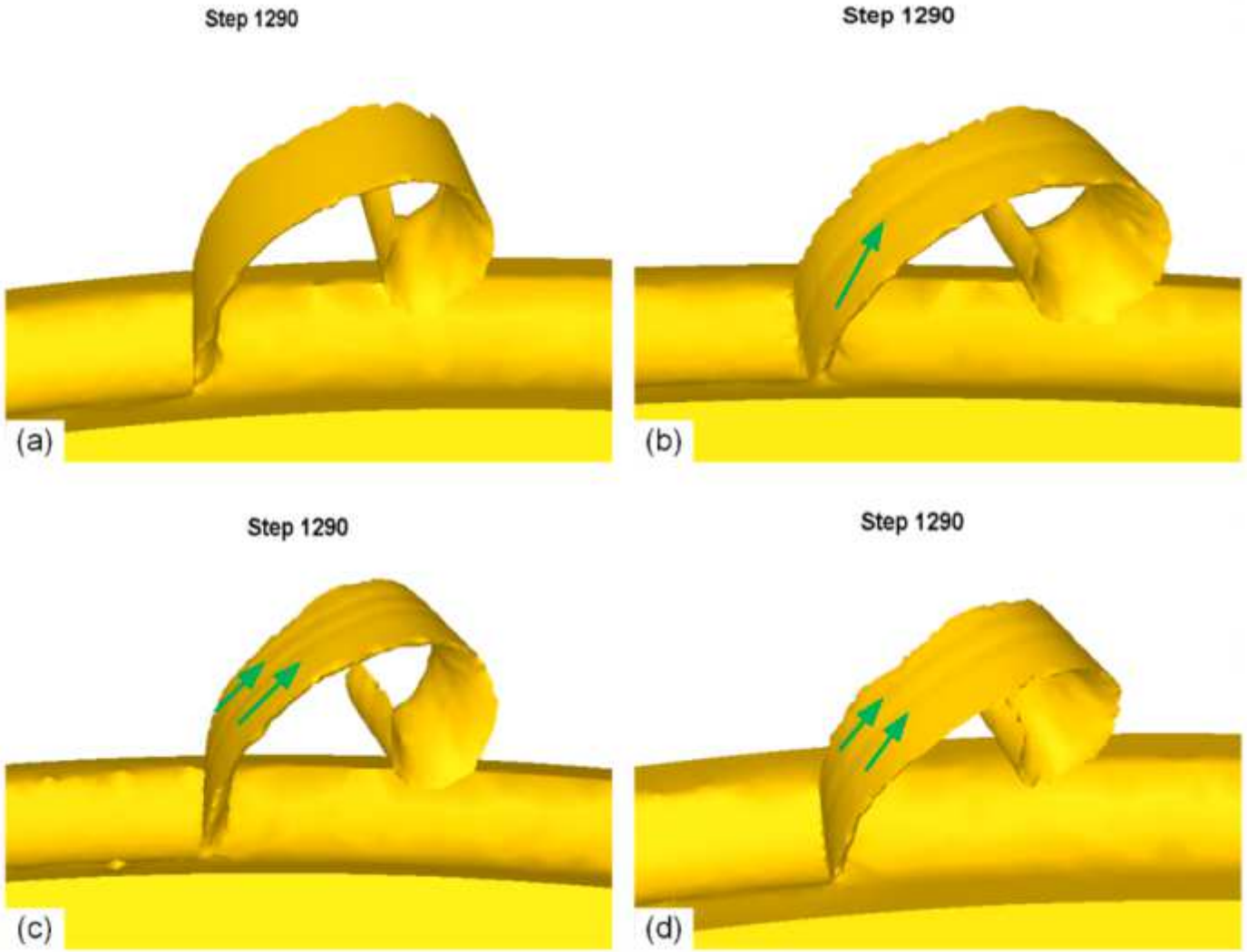

Figure 6

Chip formation of NCT (a), VCT1 (b), VCT2 (c) and VCT3 (d) tools during machining simulation at the speed of 120m/min

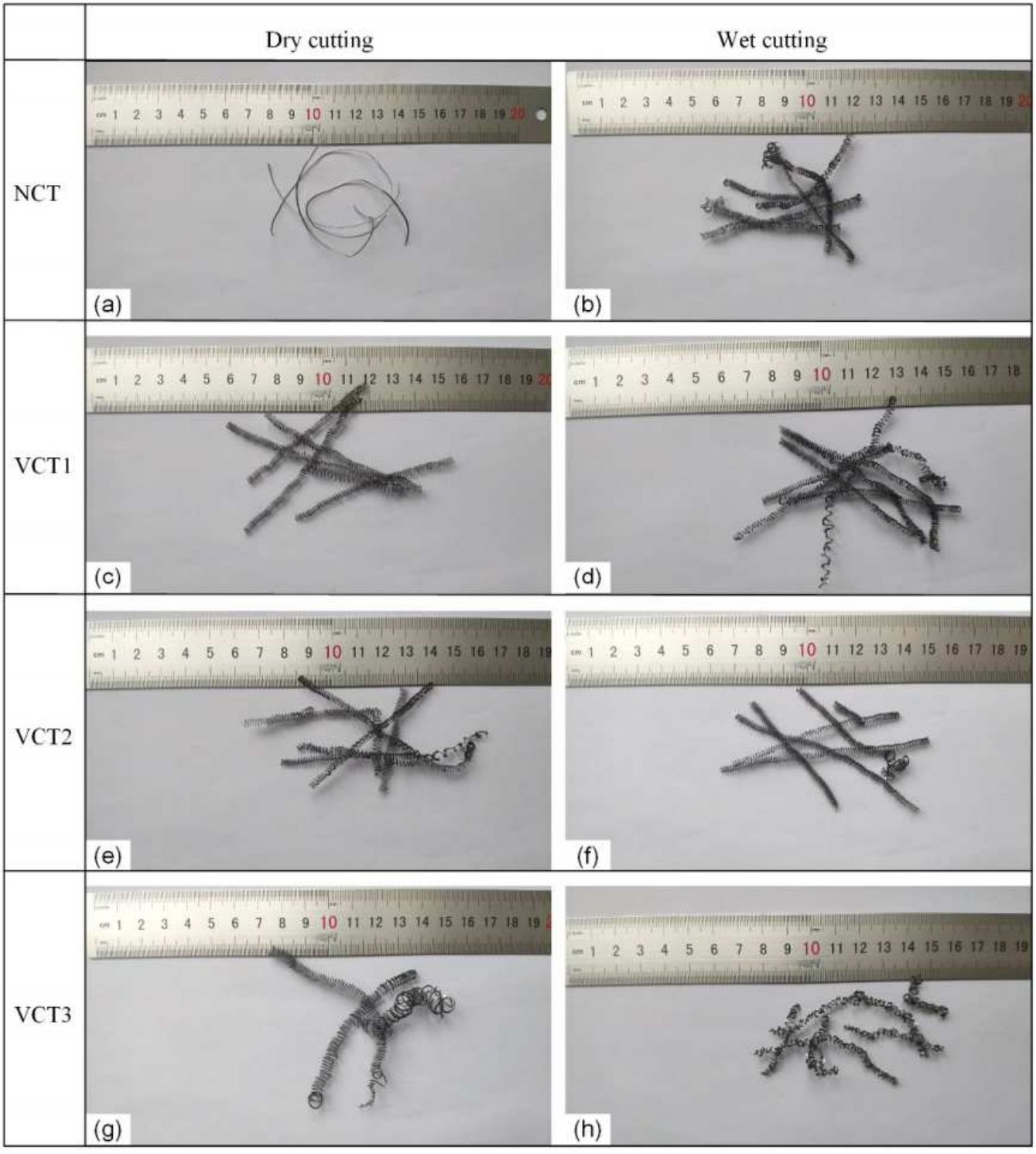

Figure 7

Chip formation of NCT (a, b), VCT1 (c, d), VCT2 (e, f) and VCT3 (g, h) tools during machining experiments at the speed of 120m/min under dry and wet conditions

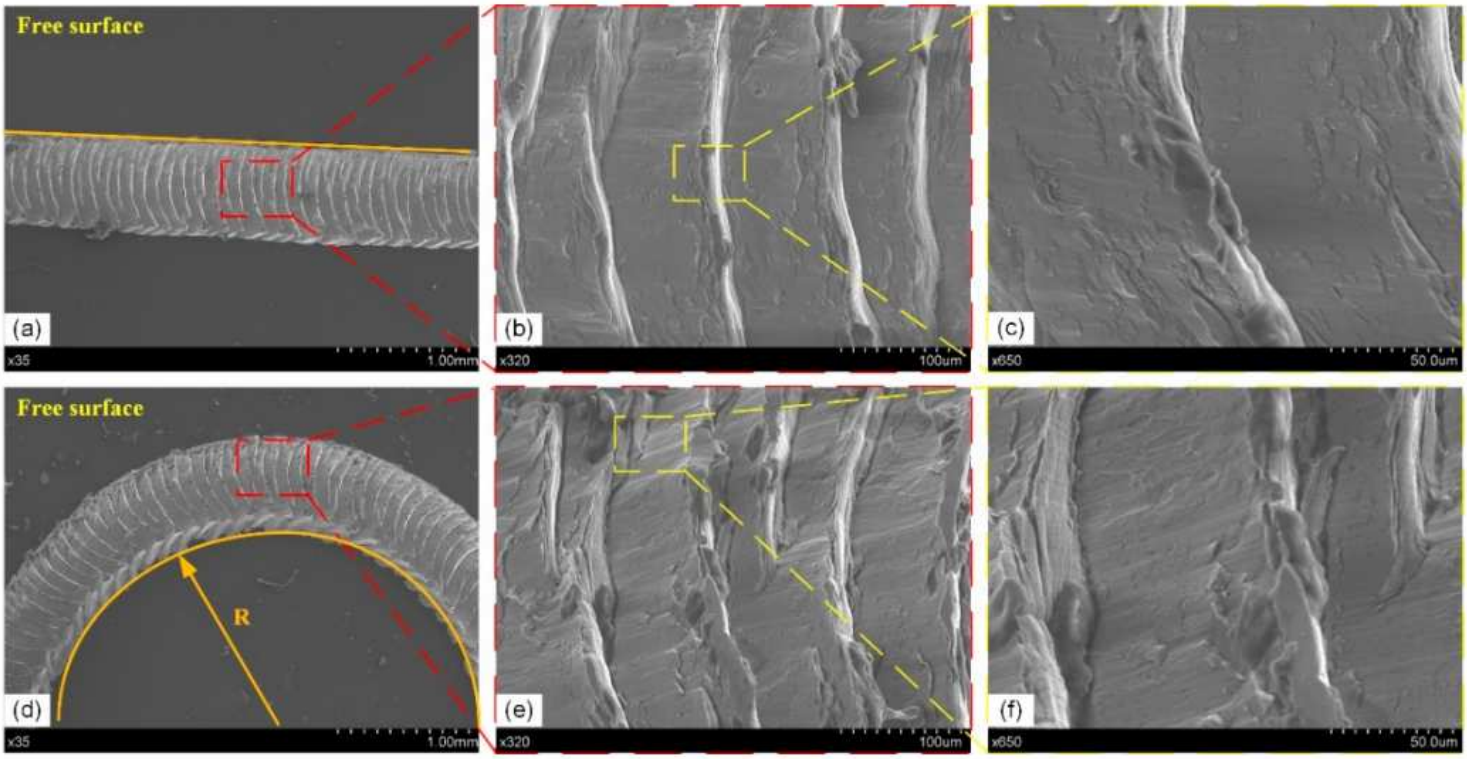

Figure 8

SEM images of chip free surface and microstructure obtained with NCT tool at the speed of 120 m/min in dry cutting (a-c) and wet cutting (d-f)

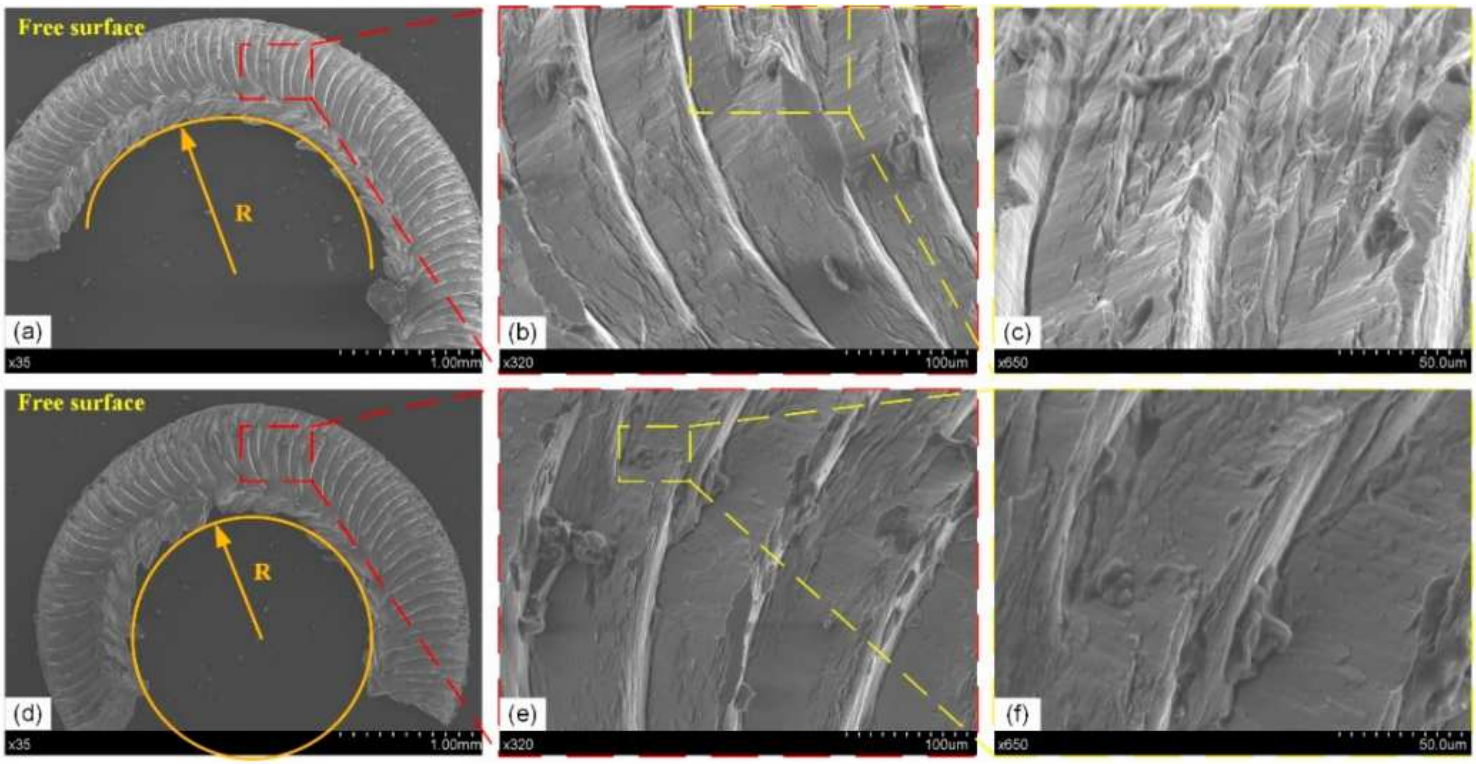

Figure 9

SEM images of chip free surface and microstructure obtained with VCT1 tool at the speed of 120 m/min in dry cutting (a-c) and wet cutting(d-f)

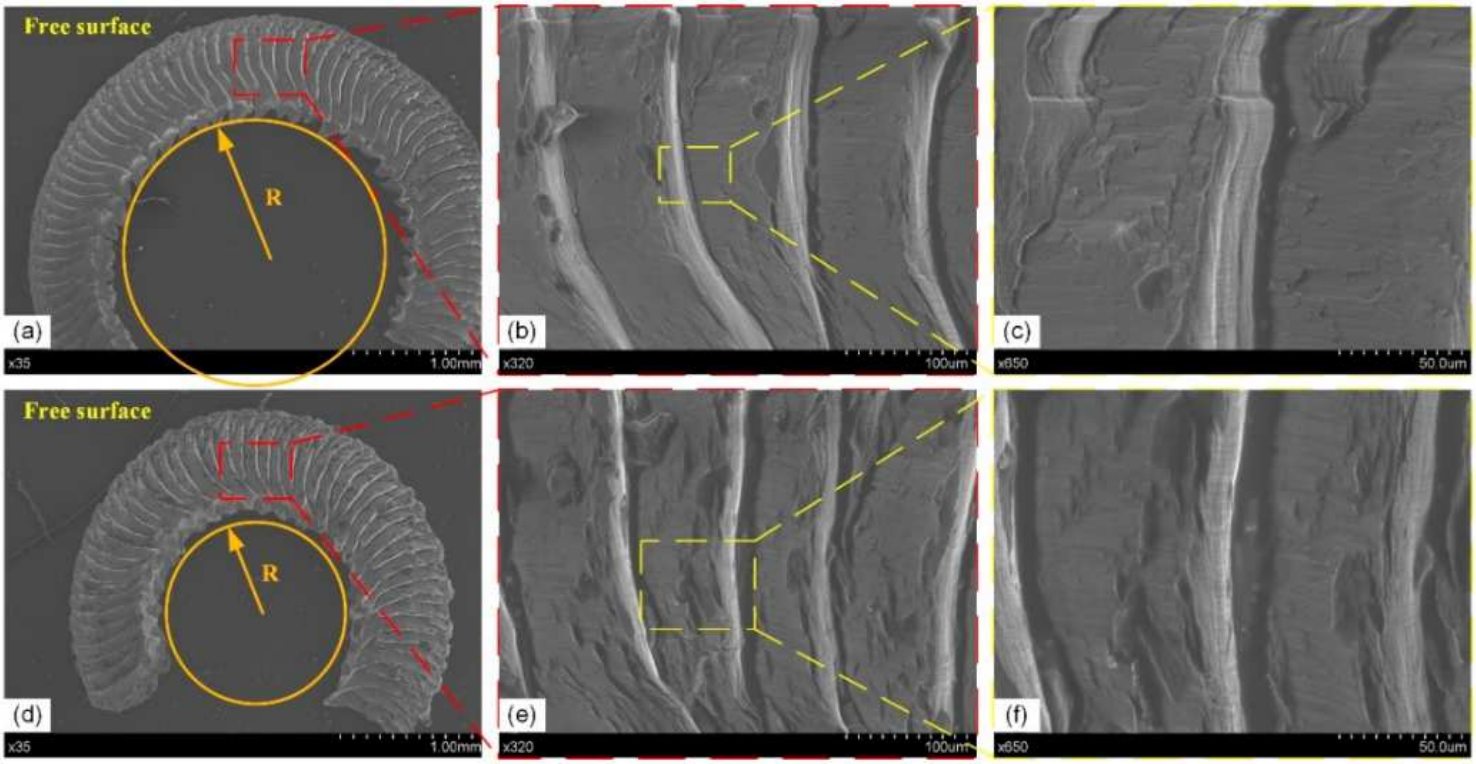

Figure 10

SEM images of chip free surface and microstructure obtained with VCT2 tool at the speed of 120 m/min in dry cutting (a-c) and wet cutting(d-f)

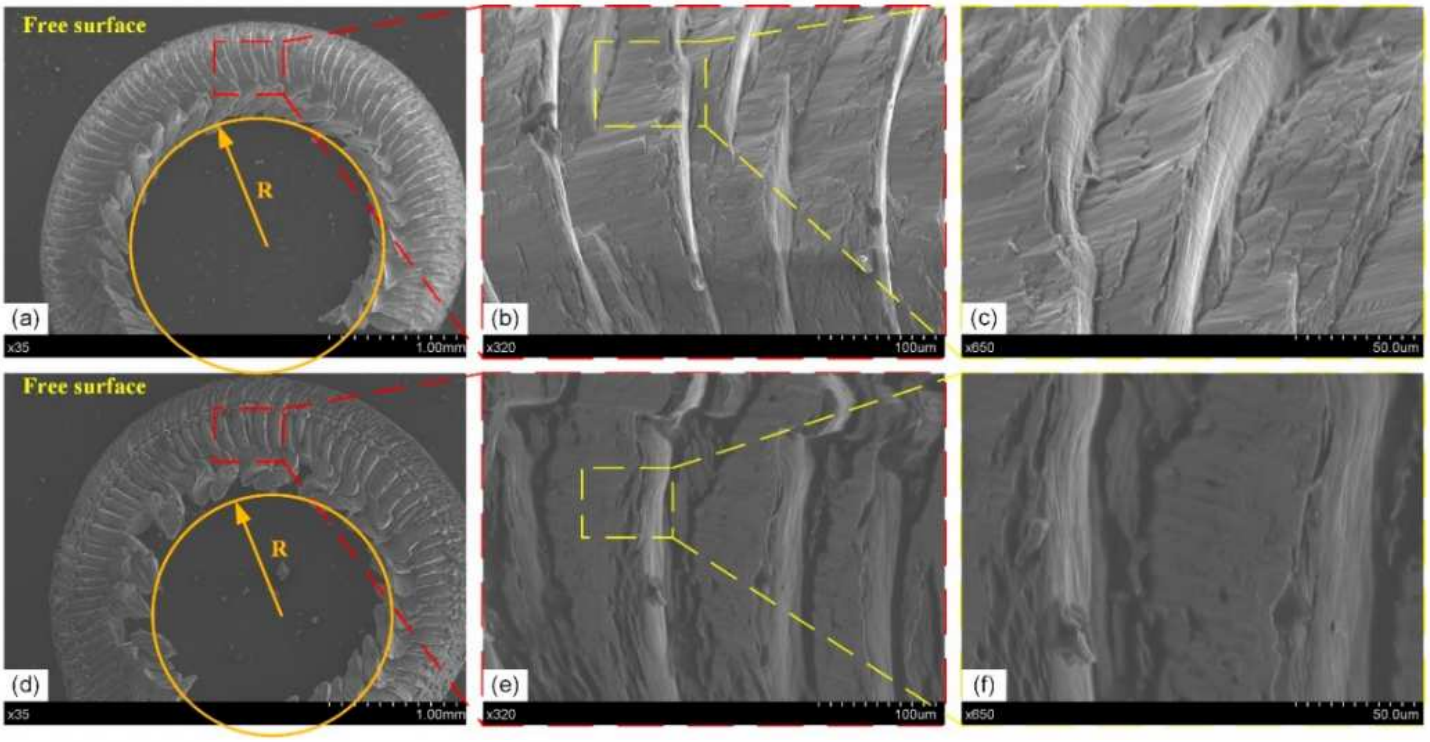

Figure 11

SEM images of chip free surface and microstructure obtained with VCT3 tool at the speed of 120 m/min dry cutting (a-c) and wet cutting(d-f)

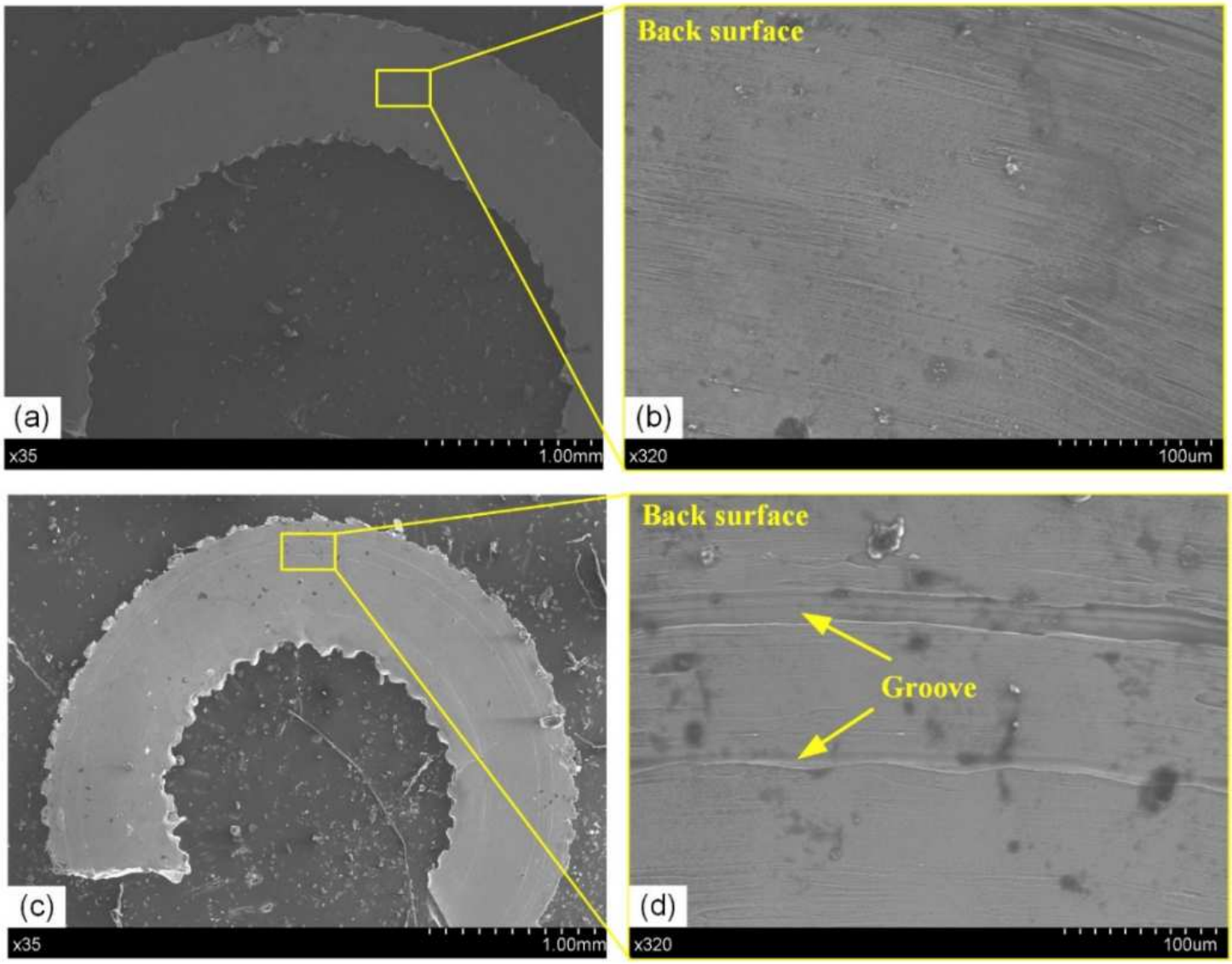

Figure 12

SEM images of chip free surface and microstructure obtained with VCT3 tool at the speed of 120 m/min dry cutting (a-c) and wet cutting(d-f)

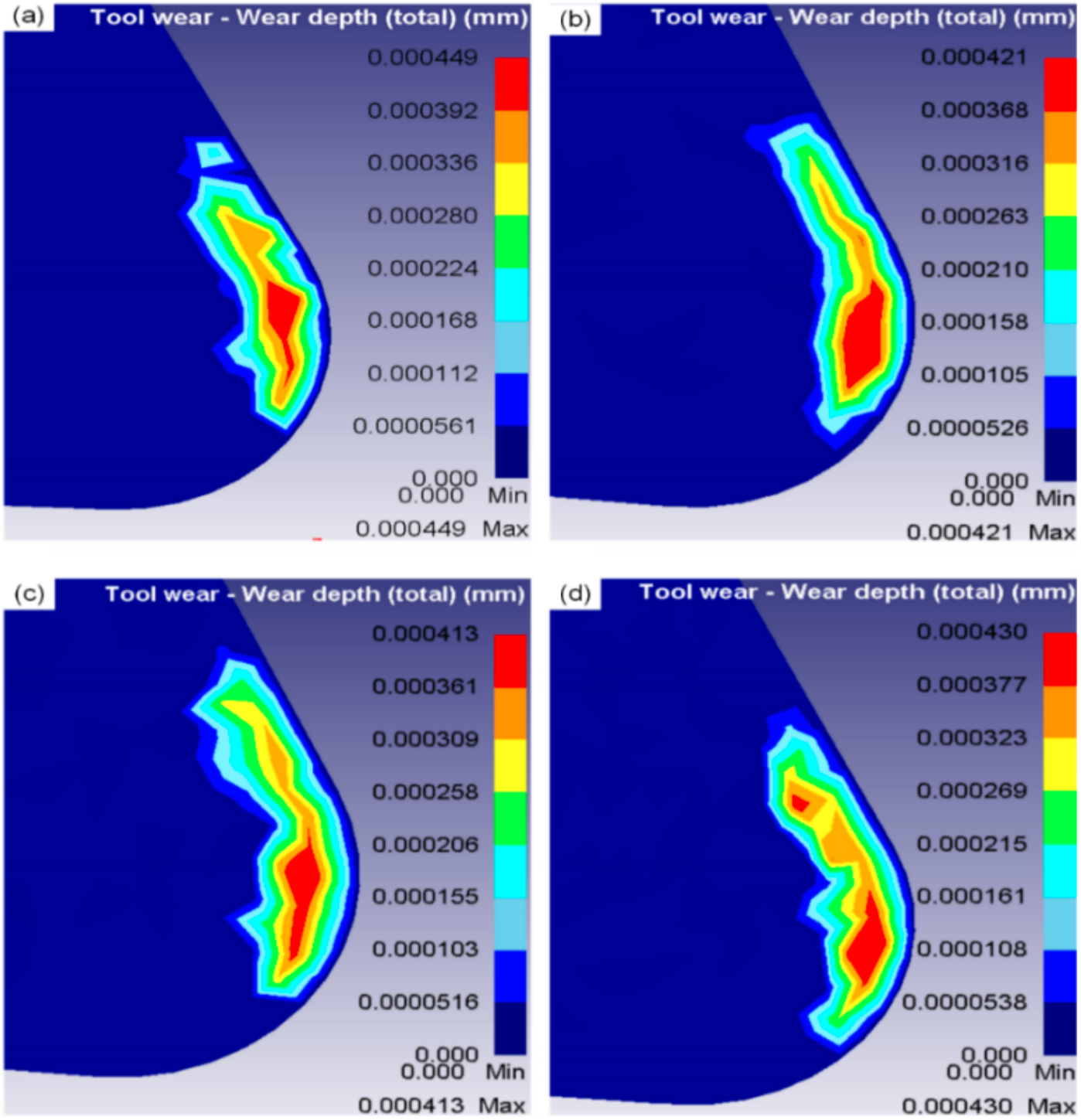

Figure 13

Wear depth of four types of cutting tools at the speed of 120m/min under simulative conditions

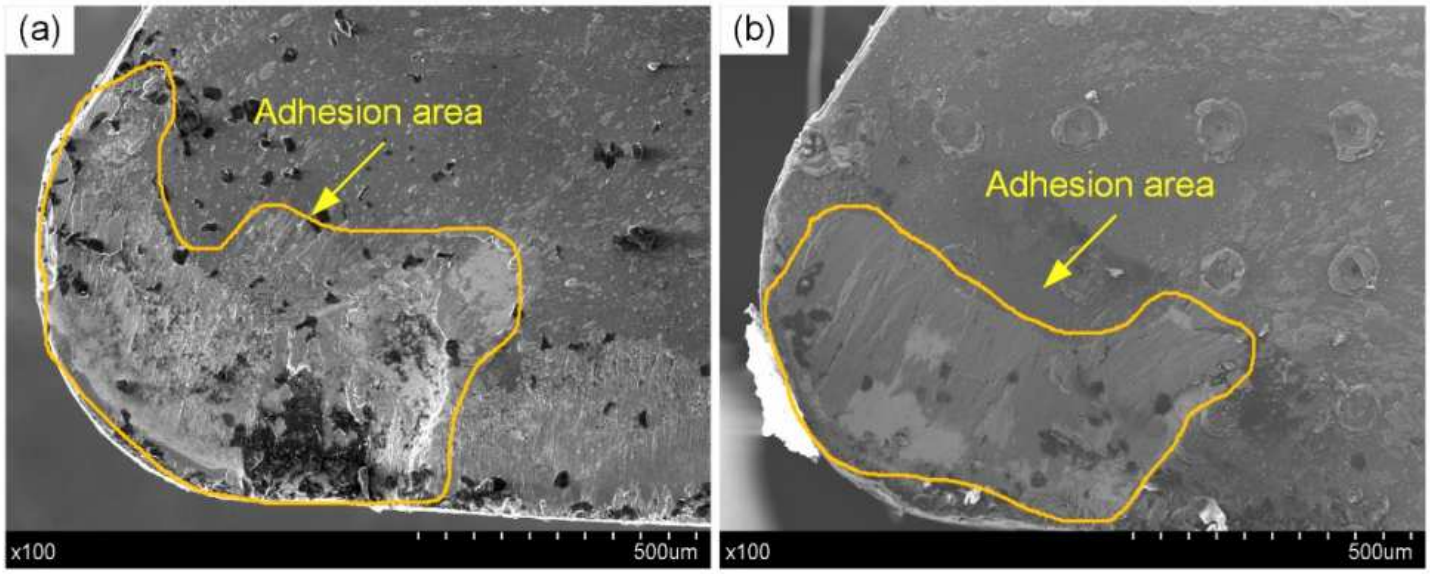

Figure 14

The marks of adhesion area on the rake face of NCT tool(a) and VCT tools (b)

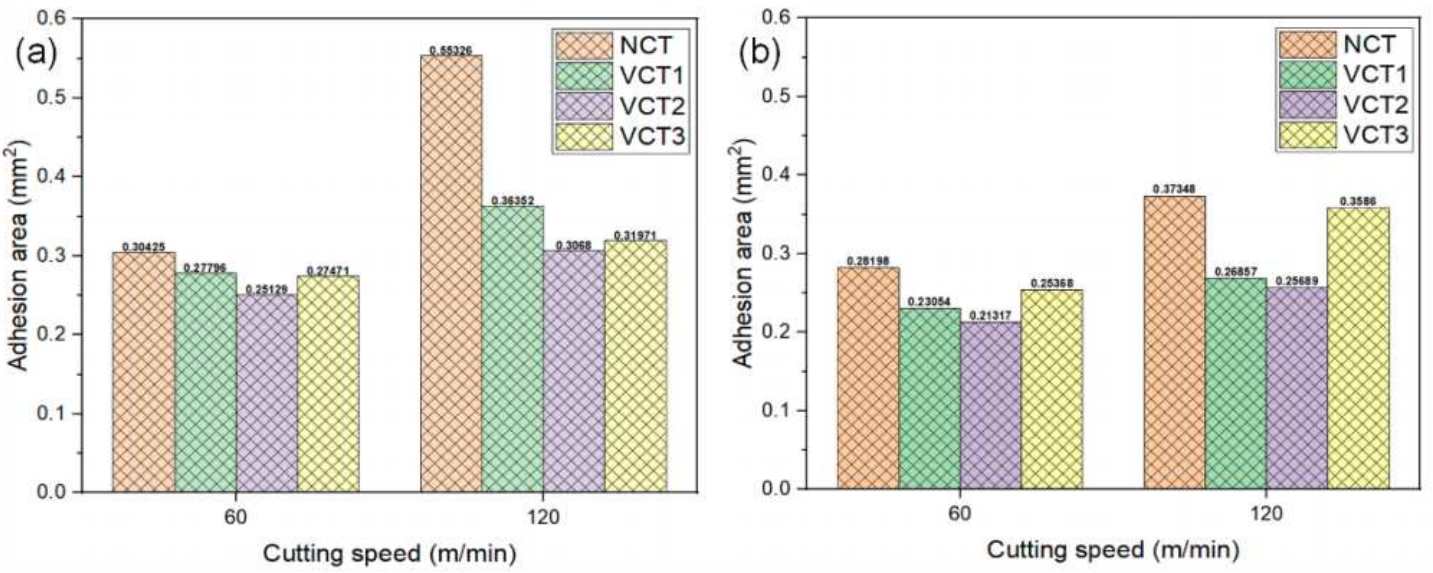

Figure 15

Adhesion area of four types of cutting tools in dry cutting (a) and wet cutting (b)

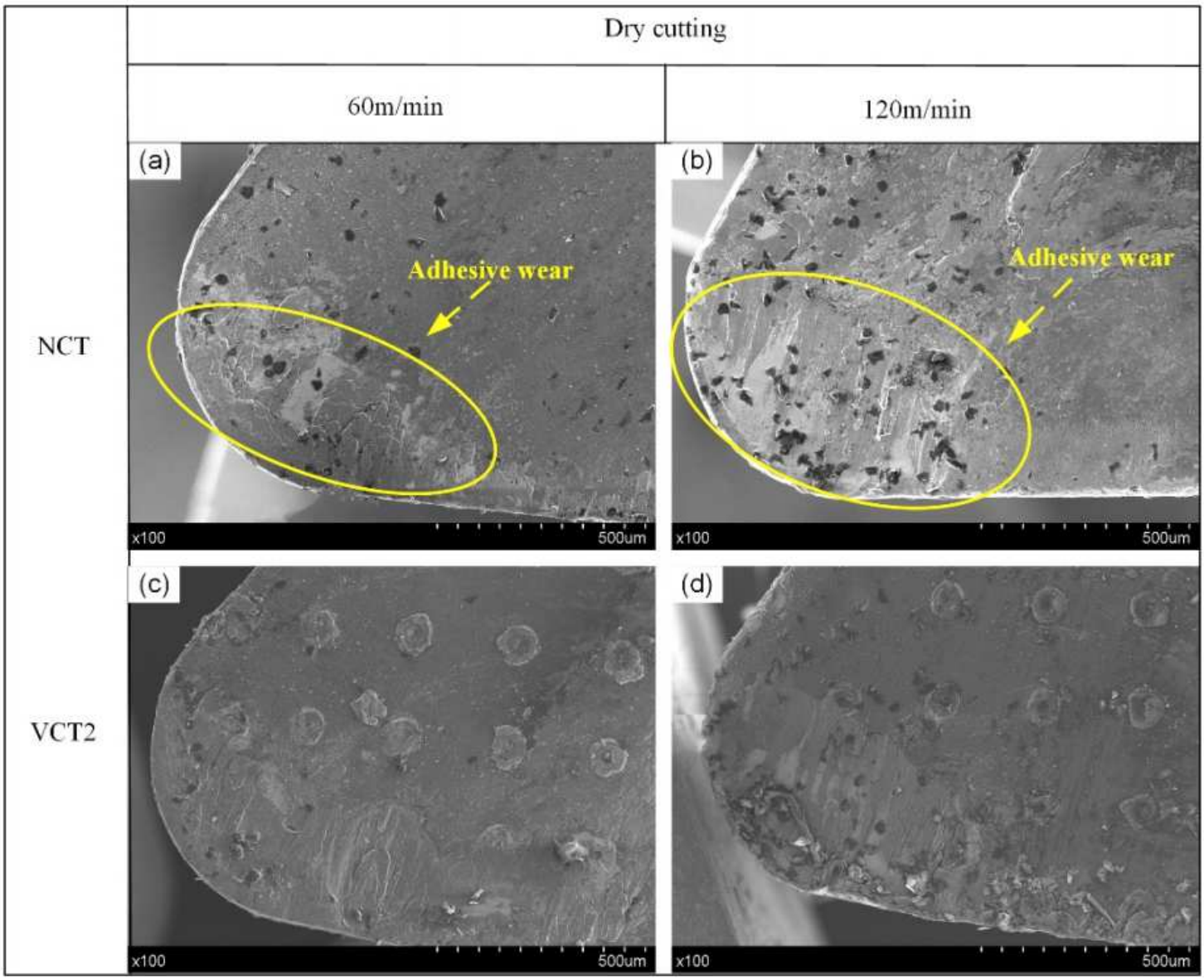

Figure 16

SEM images of wear rake face after cutting at the speed of 60m/min and 120m/min under dry cutting conditions

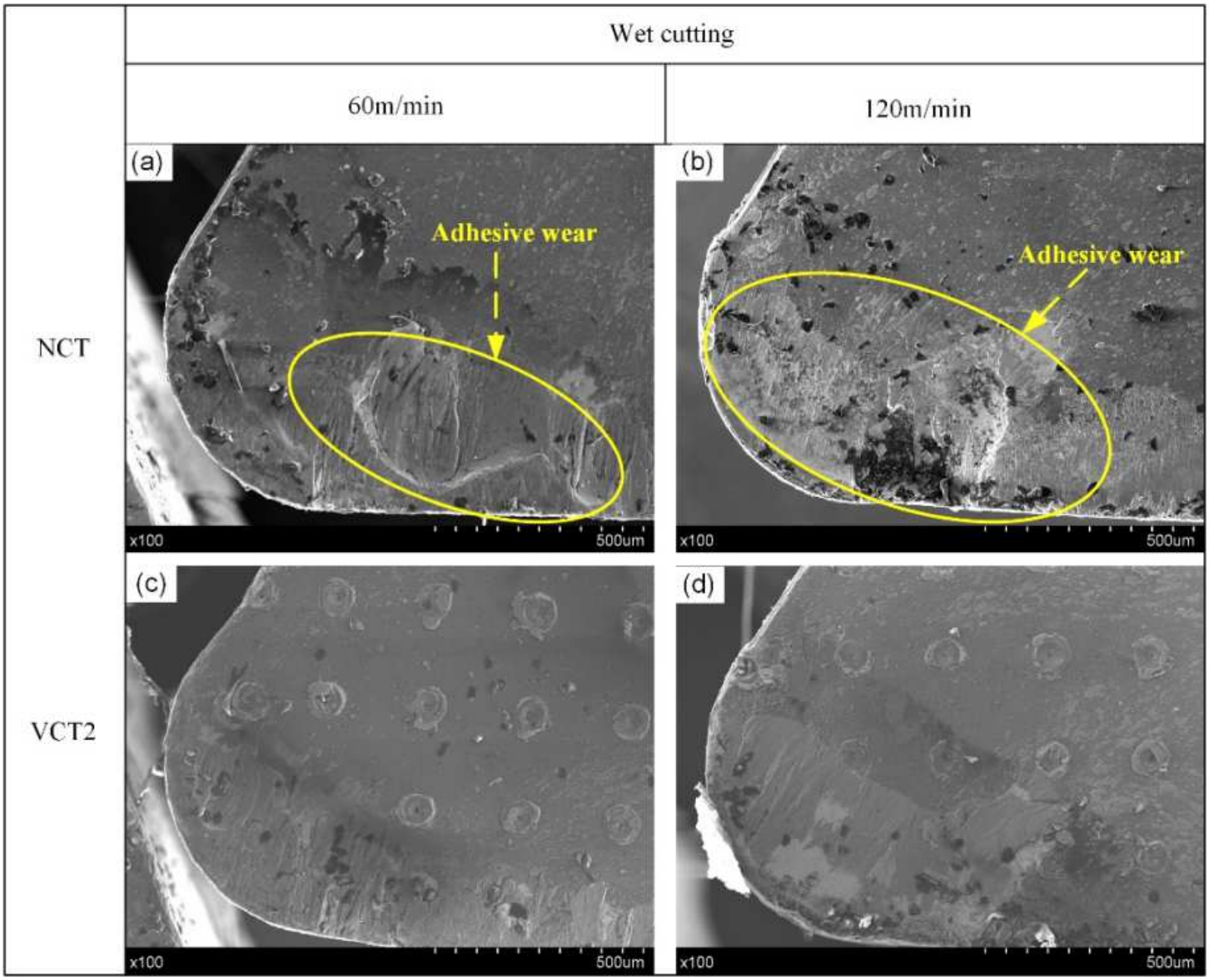

Figure 17

SEM images of wear rake face after cutting at the speed of 60m/min and 120m/min under wet cutting conditions

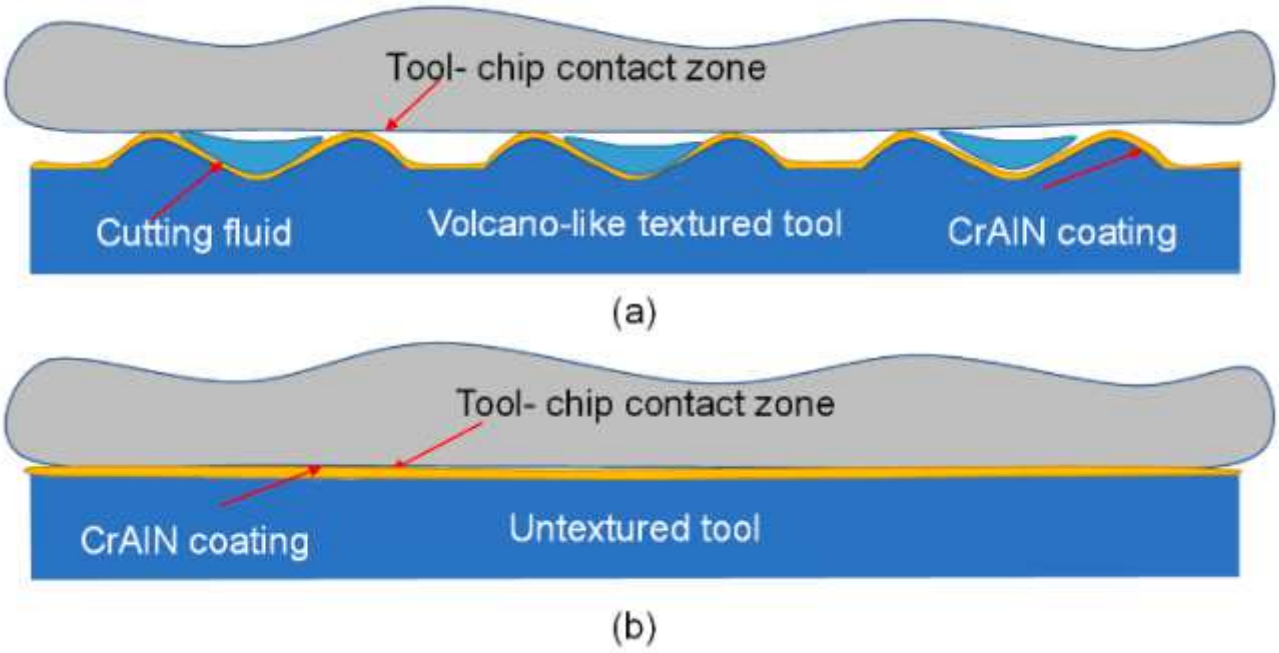

Figure 18

The schematic diagram of tool-chip contact interface

Supplementary Files

This is a list of supplementary files associated with this preprint. Click to download.

- Tables.pdf